Supplementary Material: Enhanced Ferromagnetism of CrI_3 Bilayer by Self-Intercalation

Yu Guo(郭宇), Nanshu Liu(刘南舒), Yanyan Zhao(赵艳艳), Xue Jiang(蒋雪),

Si Zhou(周思)*, and Jijun Zhao(赵纪军)

MOE Key Laboratory of Materials Modification by Laser, Ion and Electron Beams,

Dalian University of Technology, Dalian 116024, China

S1. Atomic structures of intercalated CrI_3 bilayers

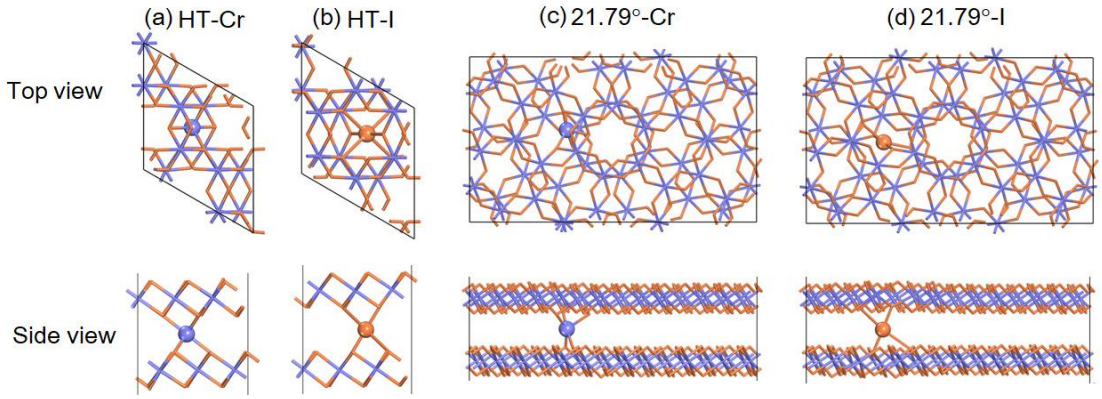

Fig. S1. Atomic structures of (a) Cr and (b) I intercalated HT phase of $\sqrt{3}\times\sqrt{3}$ supercell, and (c) Cr and (d) I intercalated twisted 21.79°-CrI_3. The Cr and I atoms are shown in purple and orange colors, respectively.

S2. The intercalation energy for intercalated bilayers

Table S1. Intercalation energy (E_{int}) for Cr and I intercalated CrI_3 bilayers in the LT and HT phases using different supercells as well as twisted bilayers.

	E_{int} (eV)	√3×√3	2×2	√7×√7	3×3	21.79°	38.42°
Cr intercalation	LT	−4.01	−4.04	−4.11	−3.97	−4.23	−3.97
	HT	−4.29	−4.30	−4.35	−4.39		
I intercalation	LT	−0.18	−0.13	−0.21	−0.31	−0.37	−0.41
	HT	−0.69	−0.75	−1.23	−1.61		

* Corresponding author. Email: sizhou@dlut.edu.cn

S3. The interlayer distance for intercalated bilayer

Table S2. Interlayer distance for Cr and I intercalated CrI_3 bilayers in the LT and HT phases using different supercells as well as twisted bilayers. The numbers in the brackets are the exchange energies for twisted 21.79°-CrI_3 and 38.42°-CrI_3 without intercalation.

	phase	pristine	√3×√3	2×2	√7×√7	3×3	21.79°	38.42°
Cr intercalation	LT	3.54	3.38	3.40	3.39	3.34	3.48 (3.64)	3.40 (3.60)
	HT	3.54	3.34	3.36	3.37	3.37		
I intercalation	LT	3.54	4.04	3.86	3.58	3.50	3.70	3.78
	HT	3.54	4.26	3.87	3.59	3.52		

S4. Thermodynamical stability of intercalated CrI_3 bilayers

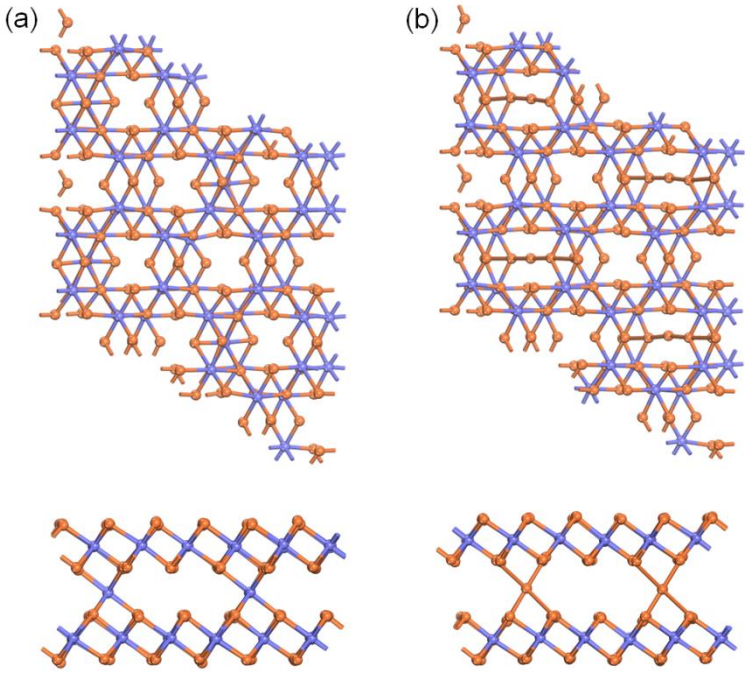

Fig. S2. Snapshots of (a) Cr and (b) I intercalated CrI_3 bilayers for HT phase from BOMD simulations with temperature controlled at 300 K. Each simulation is lasted for 10 ps.

S5. Diffusion of intercalated Cr atom at van der Waals gap

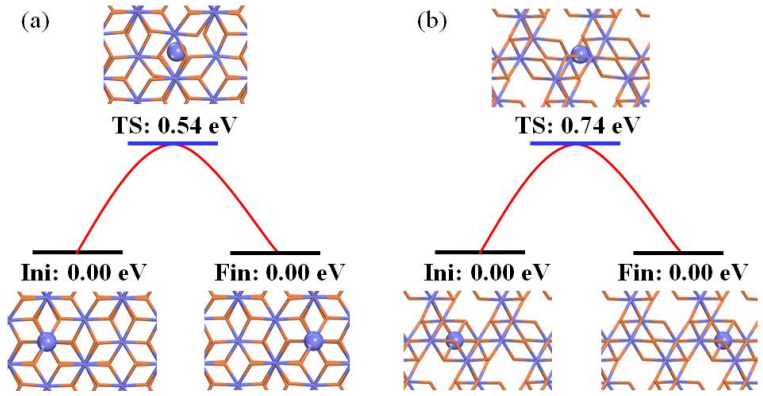

Fig. S3. Diffusion behavior of intercalated Cr atom in the van der Waals gap of (a) LT and (b) HT phases of bilayer CrI_3. The Cr and I atoms are shown in purple and orange colors, respectively. The intercalated Cr atoms are given in larger purple balls. The climbing-image nudged elastic band (CI-NEB) method was employed to investigate the diffusion kinetics and determine the activation energy for migration. Five images were used to calculate the diffusion path. The intermediate images of each CI-NEB simulation were relaxed until the perpendicular forces were smaller than 0.02 eV/Å.

S6. Exfoliation behaviors of intercalated CrI_3 systems

We calculated the exfoliation energies of intercalated and pristine CrI_3 systems by simulating the separation of one CrI_3 layer from the intercalated and pristine bilayers. The equilibrium distance between intercalated bilayer and separated layer is 3.50 Å, which can be determined by the function of distance respect to total energy (Fig. S4a). Then we simulated the exfoliation process and predicted the exfoliation energy with respect to the separation distance, as shown in Fig. S4b. The calculated exfoliation energies are 0.21 J/m^2 for pristine systems and 0.20 J/m^2 for intercalated systems, respectively, indicating that the intercalated systems preserve the exfoliation behavior of pristine layered CrI_3.

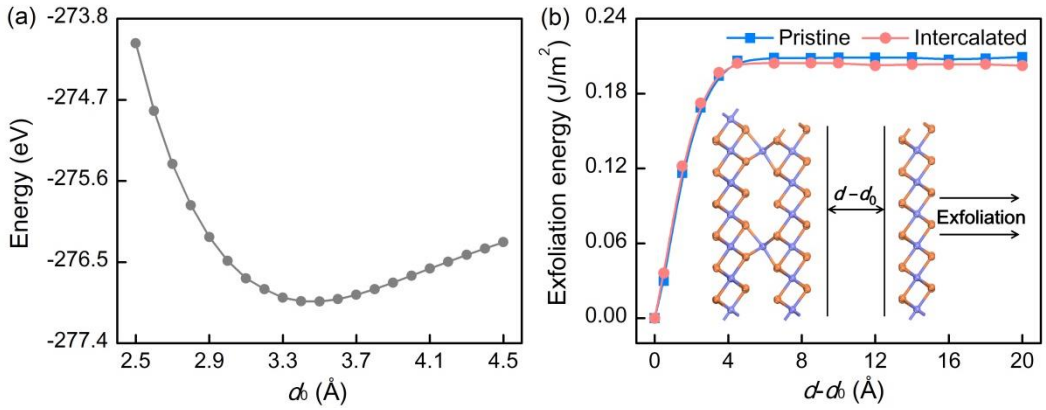

Fig. S4. (a) Total energy vs. the distance (d_0) between intercalated bilayer and a separated layer. (b) Exfoliation energy vs. separation distance d. for intercalated CrI_3 bilayer in comparison with pristine CrI_3 system.

S7. Electronic structures of intercalated bilayers

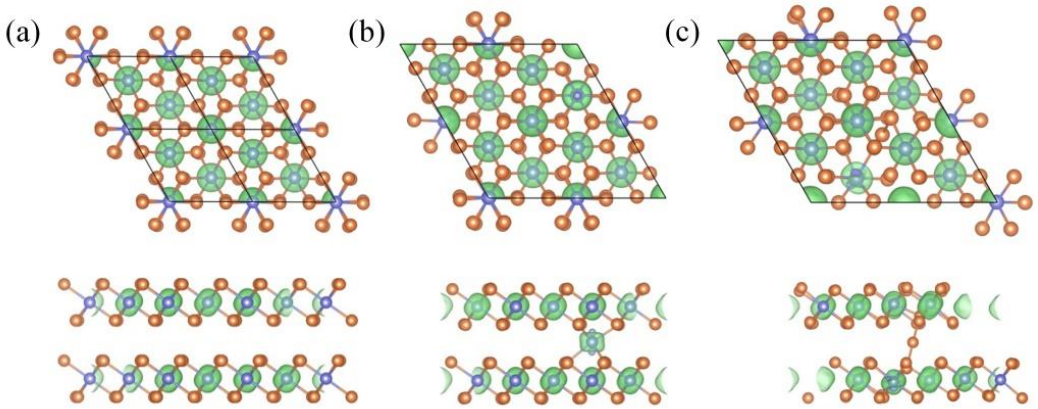

Fig. S5. Spin charge density (in green color) with an isosurface value of 0.01 e/Å^3 for (a) pristine, (b) Cr and (c) I intercalated CrI_3 bilayers, respectively. The Cr and I atoms are shown in purple and orange colors, respectively.

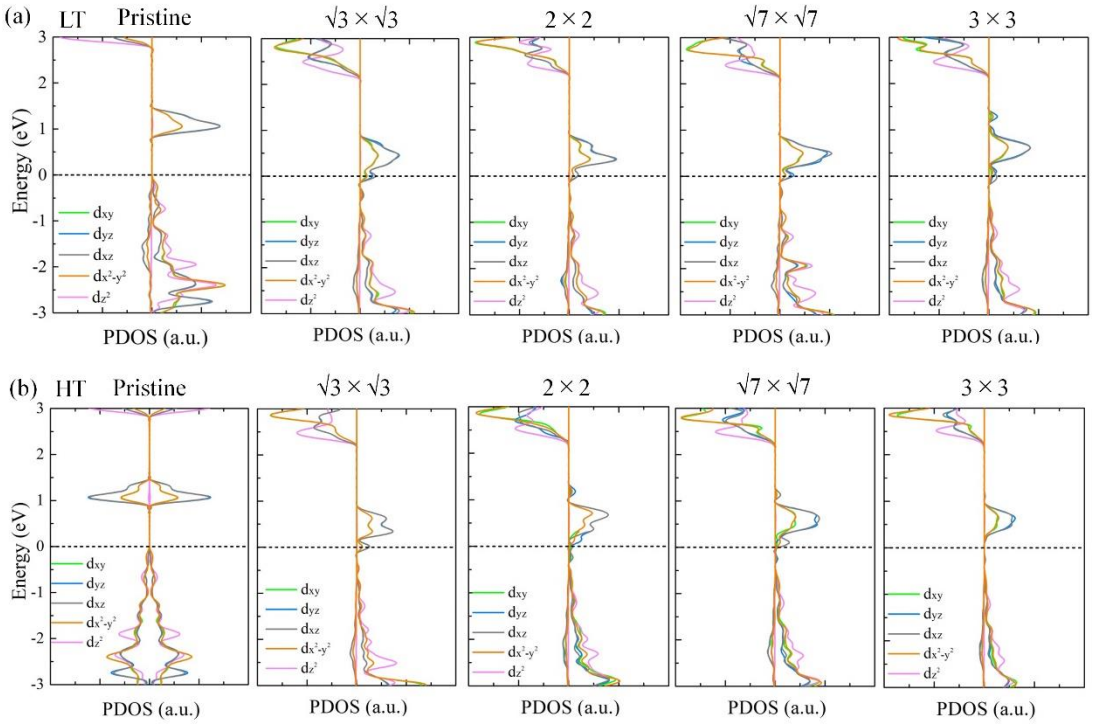

Fig. S6. Projected density of states (PDOS) of pristine and Cr-intercalated CrI_3 bilayers of (a) LT and (b) HT phases, with different supercells.

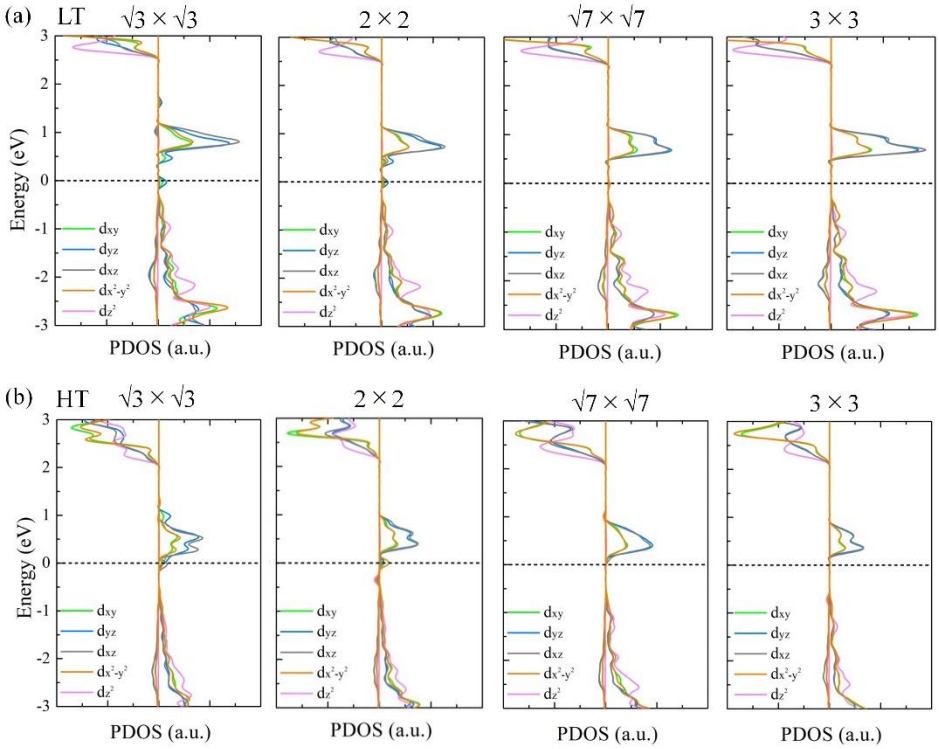

Fig. S7. Projected density of states (PDOS) of pristine and I-intercalated CrI_3 bilayers of (a) LT and (b) HT phases, with different supercells.

S8. Self-intercalation for trilayer and bulk CrI_3

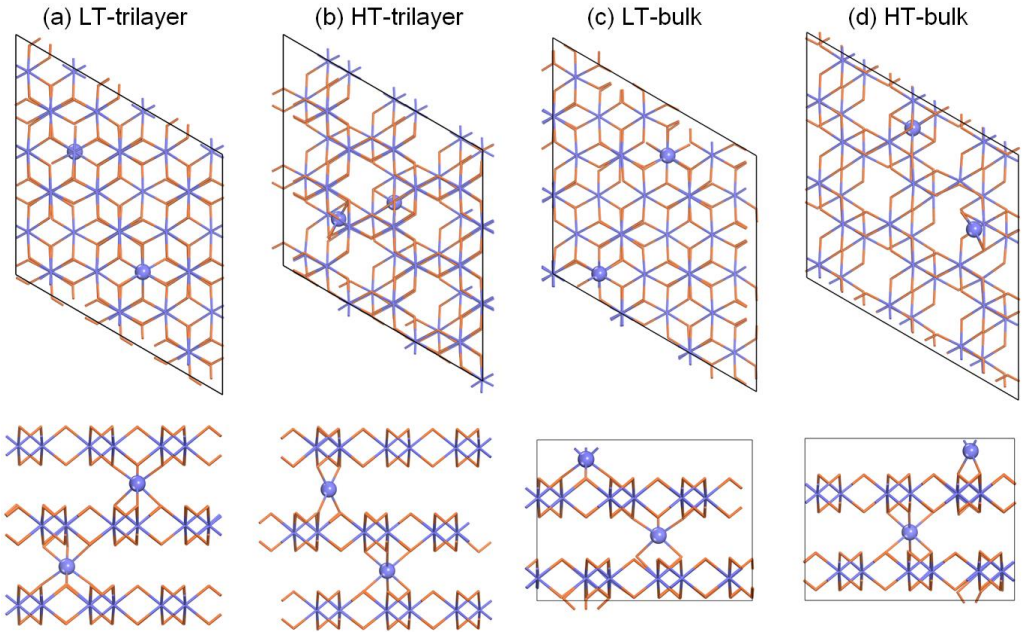

Fig. S8. Atomic structures of Cr intercalated (a) (c) LT and (b) (d) HT phases for trilayer and bulk CrI_3 in 3×3 supercell.

Table S3. Exchange energy ΔE of pristine, trilayer and bulk in LT and HT phases of 3×3 supercell. The atomic structures are shown in Fig. S8.

ΔE (meV/f.u.)	Trilayer		Bulk	
	Pristine	Intercalated	Pristine	Intercalated
LT	2.03	7.01	3.30	19.66
HT	−0.20	6.34	−0.98	13.15

S9. Virtual exchange gap for intercalated CrI_3 bilayers

Table S4. Virtual exchange gap (G_{ex}) of Cr-intercalated bilayer CrI_3 of the LT and HT phases with different supercells.

G_{ex} (eV)	pristine	√3×√3	2×2	√7×√7	3×3
LT	0.98	0.37	0.44	0.74	0.83
HT	0.92	0.48	0.59	0.76	0.81

S10. Charge transfer for the intercalated CrI_3 bilayers

Table S5. Charge transfer (CT, in the unit of electrons) of Cr and I-intercalated bilayer CrI_3 of the LT and HT phases with different supercells.

	CT (*e*)	√3×√3	2×2	√7×√7	3×3
Cr intercalation	LT	0.11	0.06	0.04	0.02
	HT	0.11	0.12	0.11	0.12
I intercalation	LT	0.08	0.06	0.07	0.06
	HT	0.10	0.06	0.11	0.11

S11. Double exchange for I-intercalated bilayers

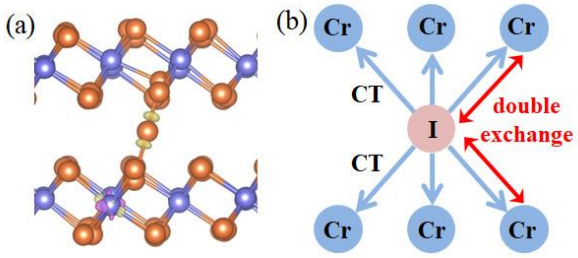

Fig. S9. Differential charge density of (a) I-intercalated LT phase of bilayer CrI_3. Yellow and pink colors represent the charge accumulation and depletion regions, respectively, with an isosurface value of 8×10^{-3} *e*/Å^3. (b) Schematic illustrations of double exchange in the I-intercalated CrI_3 bilayer. Blue arrows show the charge transfer (CT) from the intercalated I atom to the intralayer Cr atoms, and red arrows highlight the double exchange interaction between Cr-Cr atoms.